Full Paper
Journal of Nano Materials Impact 2025, 01 (01) 14-18

Nanochitosan Conjugated with Paromomycin: Preparation, Characterization and Medical Application

Hajar Falih Aldali[1], Shatha Khudiar Abbas[1], Ahmed N. Abd*[,2]
[1]Department of Biology, College of Science, Mustansiriyah University, Baghdad, IRAQ, [2]Department of Physics, College of Science, Mustansiriyah University, Baghdad, IRAQ.

Abstract
This study aims to prepare nanochitosan conjugated with paromomycin antibiotic and demonstrate its effect as a therapeutic agent against Entamoeba histolytica parasite in experimentally infected mice by studying the $CD4^+$ and $CD8^+$ lymphocyte cells. The nanomaterial was characterized using XRD examination, which indicated the formation of nanochitosan semicrystalline structure, including crystalline and amorphous. The biological results showed that $CD4^+$ $CD8^+$ had positive reactions. $CD4^+$ was the most reactive biomarker than $CD8^+$ that expresses the activation of T lymphocytes as a response to the E. histolytica infection, and these cells reduced as a response to the treatment showing the active effect of the Nanomaterial as a therapeutic agent against Entamoeba histolytica, parasite, this study is the first in its field to determine the effect of nanochitosan on lymphocytes in Entamoeba histolytica parasitic infection.

Keyword: nanochitosan • *E. histolytica* • nanomaterials • paromomycin • $CD4^+$ • $CD8^+$.

Downloaded from https://nanomatimp.uomustansiriyah.edu.iq/

Introduction

The area of nanomedicine is an evolving field that uses nanotechnology to provide new therapeutic and diagnostic approaches, understanding the structural, physical, and morphological characteristics of nanomedicines, as well as the mechanism by which they internalize inside biological systems and distribute and localize biodegradable, stabilize, and potentially have harmful health impacts, is essential for applying them in healthcare [1-3].

Since chitosan is a naturally occurring polymer with respectable mechanical stability, biodegradability, and biocompatibility, it has received considerable attention for use in gene and medication delivery systems [4]. These properties make chitosan an ideal candidate for biomedical applications, particularly in the development of nanocarriers for targeted drug delivery. Nanochitosan has shown great promise due to its enhanced surface area, improved solubility, and ability to encapsulate and deliver therapeutic agents efficiently. In the context of parasitic infections, nanochitosan has been extensively explored as both a therapeutic agent and a drug delivery vehicle. Studies have demonstrated its efficacy in enhancing the bioavailability and stability of antiparasitic drugs, reducing toxicity, and improving targeting to infected tissues [5-7].

***Address for correspondence:** Prof. Dr. Ahmed N. Abd, Department of Physics, College of Science, Mustansiriyah University, Baghdad 10052, Iraq.

E-mail: ahmed_naji_abd@uomustansiriyah.edu.iq

ORCID: https://orcid.org/0000-0003-0569-9650

This is an open access journal, and articles are distributed under the terms of the Creative Commons Attribution License (CC-BY-NC) 4.0 License, which allows others to use, distribution, and reproduction in any medium for noncommercial purposes, as long as the original work is cited properly.

Info:
Submitted: 28 Oct. 2024; **Revised:** 30 Jan. 2025;
Accepted: 2 Feb 2025; **Published:** 10 Feb 2025.
https://doi.org/10.71109/nmi.2025.1.1.5

For instance, nanochitosan-based systems have been successfully employed in the treatment of diseases caused by parasites such as Leishmania, Plasmodium, and Trypanosoma, showcasing its potential to overcome challenges associated with conventional drug delivery methods. Furthermore, the immunomodulatory properties of chitosan can synergize with its drug delivery capabilities, potentially enhancing the host's immune response against parasitic infections. These attributes highlight the significant potential of nanochitosan as a multifunctional platform for combating parasitic diseases, paving the way for innovative and effective therapeutic strategies.

Entamoeba histolytica is one of the parasites that causes mortality worldwide, with 100,000 deaths yearly [8, 9]. This parasite is the causative agent of amoebiasis, a serious public health issue in underdeveloped nations [10-12].

Experimental Part

Chitosan powder, sourced from Avonchem (United Kingdom), was utilized to prepare nanochitosan. For this, 1 g of chitosan was dissolved in 100 mL of deionized distilled water and heated to 51°C for 60 minutes. Subsequently, the solution was sonicated for 30 minutes. Additionally, Paromomycin (Humatin) capsules, manufactured by Pfizer Pharma PFE GmbH (250 mg, Germany), were diluted in distilled water at a concentration of 1 g per 100 mL. Five solutions were prepared nanochitosan, paromomycin, nanochitosan mixed with paromomycin in different levels (solution 1: 50% nanochitosan and 50% paromomycin, solution 2: 75% nanochitosan and 25% paromomycin, and solution 3: 25% nanochitosan and 75% paromomycin) after that the solutions were put in the ultrasonic bath for 30 minutes.

The X-ray diffraction (XRD) test were used to characterize the solution. Five drops from each solution were added to a heated cover slide and imaged.

Copyright © 2024 *NanoMatImp*. This work licensed under a Creative Commons Attribution Noncommercial 4.0 International License.

Parasite Collection

Parasites were isolated from 90 stool samples collected from diarrhea patients at Emam Ali (A) Hospital in Iraq between June and July 2022. The identification of *E. histolytica* trophozoites and cysts was conducted following the methodology outlined in [13, 14], utilizing direct saline mounts and Lugol's iodine wet mounts for each sample. Subsequently, the samples were subjected to an ultrasonic bath for 30 minutes.

Experiment Model

Seventy Swiss albino male mice were used; their age was 6 to 14 weeks, and they weighed 25 to 30 g. All mice were housed in hygienic plastic cages that included special mice diets and sterile water. Mice stool was checked to ensure they did not have intestinal parasites before the experiment, and all groups except the control negative got daily oral cyclosporine (Sandimmune) (0.2 ml/mouse) to suppress their immune systems for 2 days. Then, all groups except the normal control were orally infected with E. histolytica trophozoites (10^3 cell/ mL).

Experiment Design

The experimental design involved seven groups, each consisting of 10 mice. All groups, except the negative control, were infected with E. histolytica trophozoites at a concentration of 1×10^3 cells/mL. The negative control group was orally administered 0.2 mL of normal saline only, while the positive control group was infected with the parasite but received no treatment. Group 1 (G1) was infected and treated with 0.2 mL of nanochitosan, and Group 2 (G2) was infected and treated with 0.2 mL of paromomycin antibiotic. Groups 3, 4, and 5 (G3, G4, and G5) were infected and treated with 0.2 mL of solution 1, solution 2, and solution 3, respectively

Determination of $CD4^+$ and $CD8^+$ lymphocytes

FLEX monoclonal mouse anti human $CD4^+$ clone 4B12 kit, (Dako Denmark) was used to determine the $CD4^+$ and FLEX monoclonal mouse anti human $CD8^+$ clone C8/144B kit, (Dako Denmark) was used to determine the $CD8^+$

Results and Discussion

X-ray Diffraction (XRD) Measurements

Scientists and researchers often analyze the X-ray diffraction (XRD) patterns of chitosan to study its crystallinity, as this property significantly influences the material's mechanical and thermal characteristics, as well as its suitability for various applications in fields such as food science, pharmaceuticals, and biomedicine. Figure 1 presents the XRD patterns of chitosan and chitosan-Paromomycin, revealing a distinct peak at approximately 2θ≈20˚, which is characteristic of chitosan' s crystalline structure. The broad nature of this diffraction peak typically reflects chitosan's semi-crystalline composition, consisting of both crystalline and amorphous regions. Factors such as processing conditions, molecular weight, and the degree of deacetylation can influence chitosan's crystallinity, while the peak's broadness indicates a diversity of crystal sizes and orientations within the material.

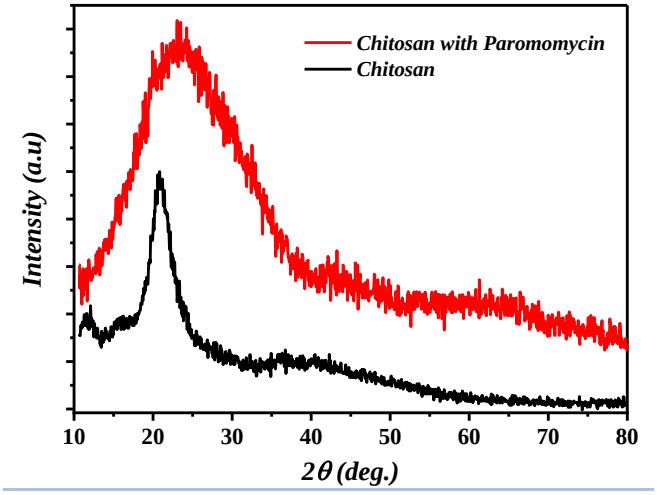

Figure 1. XRD patterns of chitosan nanoparticles and nanochitosan-Paromomycin composite nanoparticles.

Furthermore, the incorporation of paromomycin into the chitosan matrix resulted in a broader peak (red curve) at the same position as observed in pure chitosan. This broadening of the XRD peak suggests that paromomycin becomes intercalated within the chitosan matrix, altering its crystalline structure. This finding aligns with the results reported by [15-17]. The crystallite size (D) of the samples was determined using the Debye-Scherer formula[18]:

$$D = 0.9\lambda/\beta \cos\theta \quad \text{... (1)}$$

Here, β represents the Full Width at Half Maximum (FWHM), measured in radians. The crystallite size of chitosan was calculated to be approximately 4 nm, which is larger than that of chitosan with paromomycin, measured at around 2 nm.

Immunohistochemically study of the colon

T lymphocytes, or T cells, are the primary components of the adaptive immune system and play a critical role in maintaining health and defending against diseases. T cell development occurs in the thymus through a stepwise process, primarily generating $CD4^+$ and $CD8^+$ T cell subsets. These subsets are responsible for long-term immunity, immune regulation, and direct cell-mediated killing [19]. During parasitic infections, $CD4^+$ T lymphocytes and their unique cell surface proteins play a more prominent role in cellular defense, while $CD8^+$ T lymphocytes have a relatively minor function [20].

In the experimentally infected mice, both CD4+ and CD8+ cells exhibited positive responses, with CD4+ emerging as the most reactive biomarker, indicating T lymphocyte activation in response to *E. histolytica* infection. When comparing the positive and negative control groups, the positive control showed significantly higher levels of CD4+

Downloaded from https://nanomatimp.uomustansiriyah.edu.iq/

Copyright © 2024 *NanoMatImp*. This work licensed under a Creative Commons Attribution Noncommercial 4.0 International License.

expression and lower levels of CD8+ expression, as illustrated in **Figures 2 – Figure 4**.

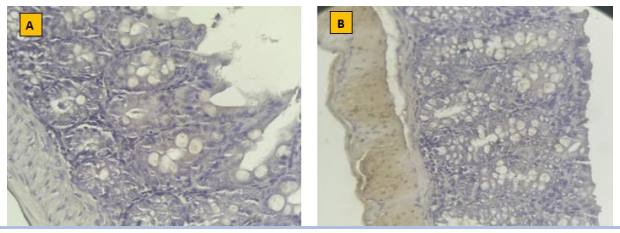

Figure 2. Immunohistochemical staining of colon of control negative showing normal histological appearance. A CD4 marker, X40 & B CD8 marker X10.

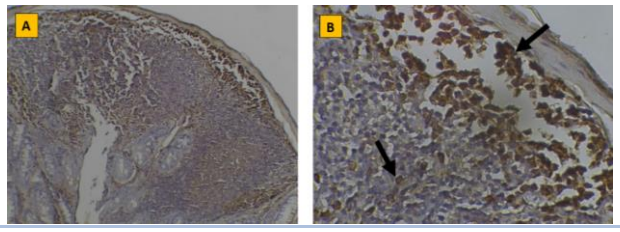

Figure 3. Immunohistochemical staining of CD4 of colon of control positive showing positive T lymphocytes (CD4) aggregation (black arrow). A X10 & B X40.

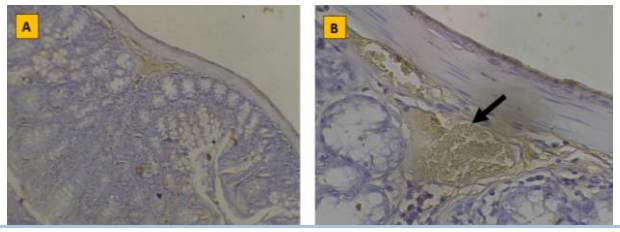

Figure 4. Immunohistochemical staining of CD8 of colon of control positive showing positive T lymphocytes (CD8) aggregation (black arrow). A X10 & B X40.

When comparing all treated groups with the positive control, a decrease in the number of $CD4^+$ and $CD8^+$ lymphocytes was noted after 7 days of treatment (**Figure 5 – Figure 14**).

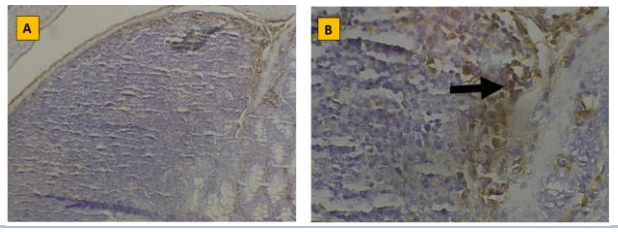

Figure 5. Immunohistochemical staining of CD4 of colon of G1 showing lymphocyte aggregation (black arrow) AX10 & BX40.

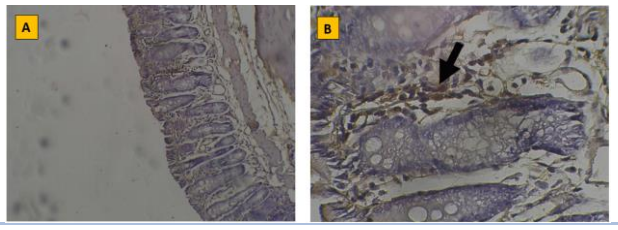

Figure 6. Immunohistochemical staining of CD8 of colon of G1 showing lymphocyte aggregation (black arrow) AX10 & BX40.

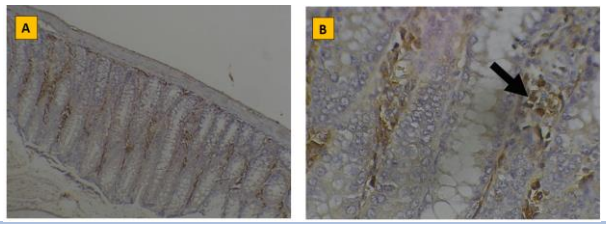

Figure 7. Immunohistochemical staining of CD4 of the colon of G2 showing lymphocyte infiltration (black arrow). A X10 & B X40.

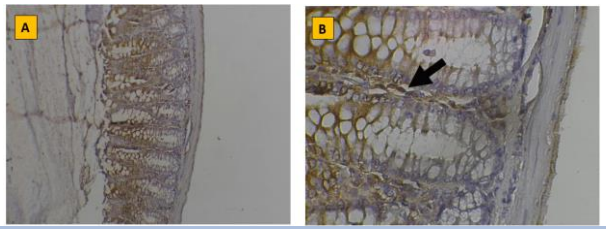

Figure 8. Immunohistochemical staining of CD8 of the colon of G2 showing lymphocyte infiltration (CD8) (black arrow). A X10 & B X40.

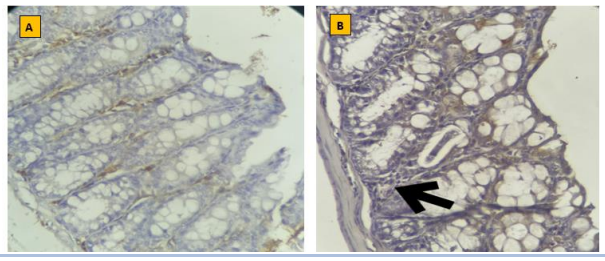

Figure 9. Immunohistochemical staining of CD4 of colon of G3 showing neutrophils infiltration (black arrow). AX10 & BX40.

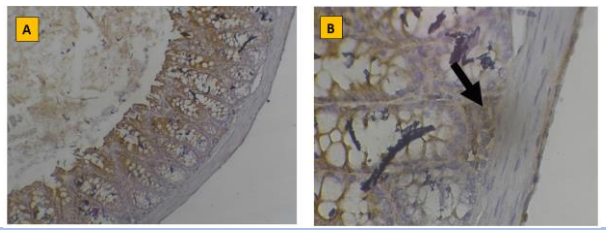

Figure 10. Immunohistochemical staining of CD8 of colon of G3 showing lymphocytes infiltration (black arrow). A X10 & B X40.

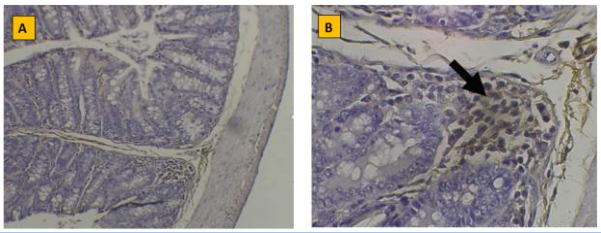

Figure 11. Immunohistochemical staining of CD4 of the colon of G4 showing goblet cell hyperplasia (red arrow) and lymphocyte positive cell aggregation (black arrow) AX10 & BX40.

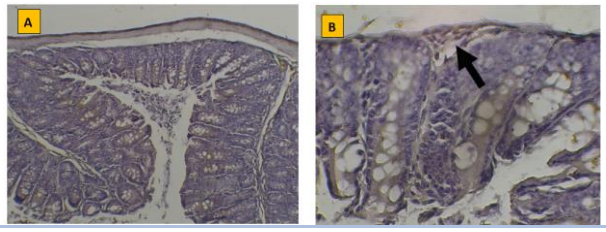

Figure 12. Immunohistochemical staining of CD8 of the colon of G4 showing lymphocyte positive cell (CD8) aggregation (black arrow) AX10 & BX40.

Downloaded from https://nanomatimp.uomustansiriyah.edu.iq/

Copyright © 2024 *NanoMatImp*. This work licensed under a Creative Commons Attribution Noncommercial 4.0 International License.

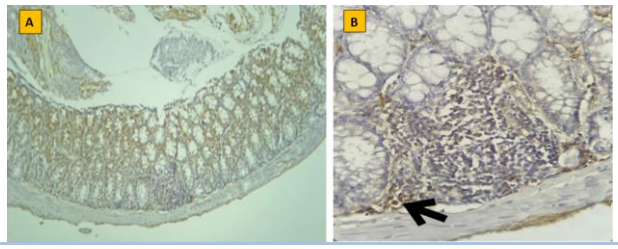

Figure 13. Immunohistochemical staining of CD4 of colon of G5 showing T lymphocytes (CD4) aggregation (black arrow). A X10 & B X40.

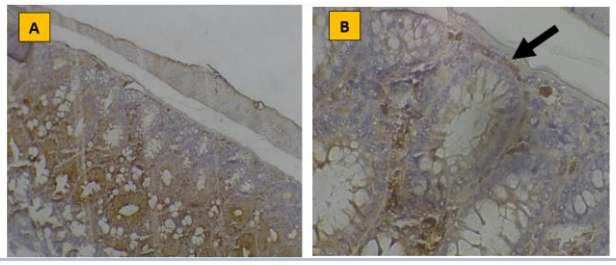

Figure 14. Immunohistochemical staining of CD8 of colon of G5 showing T lymphocytes (CD8) aggregation (black arrow). A X10 & B X 40.

For $CD4^+$ T cells, the most significant decrease was observed in the G3 group (Figure 9), whereas the G5 group maintained a high number of these cells (Figure 13). In contrast, $CD8^+$ lymphocytes did not show significant changes except in the G3 group (Figure 10).

To the best of our knowledge, there are limited and brief studies that have immunohistochemically examined $CD4^+$ and $CD8^+$ T cells in the colon during *E. histolytica* infections. The immunohistochemical analysis of mice samples infected with *E. histolytica* revealed that $CD4^+$ T cells were the predominant cell type infiltrating the tissue. This finding aligns with results reported in several previous studies [21, 22].

Conclusion

the analysis of XRD patterns provides valuable insights into the crystallinity of chitosan with crystallite size from approximately 2 nm in pure chitosan to around 4 nm in the chitosan-Paromomycin composite. These findings highlight the significant influence of processing conditions, molecular interactions, and additive incorporation on the crystallinity of chitosan, which in turn affects its mechanical, thermal, and functional properties. Such insights are crucial for optimizing chitosan-based materials for diverse applications in food science, pharmaceuticals, and biomedicine, where tailored crystallinity can enhance performance and suitability for specific uses. While there are limited and brief studies investigating the immunohistochemical presence of CD4+ and CD8+ T cells in the colon during *E. histolytica* infections, the analysis of infected mice samples revealed that CD4+ T cells are the predominant cell type infiltrating the tissue. This observation is consistent with findings from previous studies, underscoring the critical role of CD4+ T cells in the immune response to *E. histolytica* infection. This study concluded that nanochitosan conjugated with paromomycin is potentially effective as it significantly reduced the $CD4^+$ and $CD8^+$ T cells in experimentally infected mice.

Acknowledgements

The authors would like to express their thanks and gratitude to Department of Physics and Department of Biology, College of Science, Mustansiriyah, University, Iraq.

Declaration of Competing Interests

The authors declare that they have no conflicts of interest

References

[1] Z. Pei *et al.*, "Current perspectives and trend of nanomedicine in cancer: A review and bibliometric analysis," *Journal of Controlled Release*, vol. 352, p. 211-241, 2022. https://doi.org/10.1016/j.jconrel.2022.10.023.

[2] T. Lammers, "Nanomedicine Tumor Targeting," *Advanced Materials*, vol. 36, no. 26, p. 2312169, 2024. https://doi.org/10.1002/adma.202312169.

[3] P. Gupta, N. Rai, A. Verma, and V. Gautam, "Microscopy based methods for characterization, drug delivery, and understanding the dynamics of nanoparticles," *Medicinal Research Reviews*, vol. 44, no. 1, p. 138-168, 2024. https://doi.org/10.1002/med.21981.

[4] M. Saeedi *et al.*, "Customizing nano-chitosan for sustainable drug delivery," *Journal of Controlled Release*, vol. 350, p. 175-192, 2022. https://doi.org/10.1016/j.jconrel.2022.07.038.

[5] S. Bahrami, S. Esmaeilzadeh, M. Zarei, and F. Ahmadi, "Potential application of nanochitosan film as a therapeutic agent against cutaneous leishmaniasis caused by L. major," *Parasitology Research*, vol. 114, no. 12, p. 4617-4624, 2015. https://doi.org/10.1007/s00436-015-4707-5.

[6] T. Elmi *et al.*, "In Vitro Antiprotozoal Effects of Nano-chitosan on Plasmodium falciparum, Giardia lamblia and Trichomonas vaginalis," *Acta Parasitologica*, vol. 66, no. 1, p. 39-52, 2021. https://doi.org/10.1007/s11686-020-00255-6.

[7] M. A. El-sheikh, A. Badry, I. M. M. Gobaara, and A. Abd El-Aziz, "2-In vitro Scolecidal Effects of Chitosan (isolatedfrom some scorpions), Chitosan Nanoparticles, Scorpion'S Venom, and Scorpion Venom-Loaded Chitosan Nanoparticles," *Egyptian Academic Journal of Biological Sciences, B. Zoology*, vol. 15, no. 1, p. 1-17, 2023. https://doi.org/10.21608/eajbsz.2023.279995.

[8] C. H. Chang, W. C. See Too, B. H. Lim, and L. L. Few, "Identification and Characterization of Entamoeba histolytica Choline Kinase," *Acta Parasitologica*, vol. 69, no. 1, p. 426-438, 2024. https://doi.org/10.1007/s11686-023-00763-1.

[9] N. Jasni, S. Saidin, W. W. Kin, N. Arifin, and N. Othman, "Entamoeba histolytica: Membrane and Non-Membrane Protein Structure, Function, Immune Response Interaction, and Vaccine Development," *Membranes*, vol. 12, no. 11, p. 1079, 2022. https://doi.org/10.3390/membranes12111079.

Downloaded from https://nanomatimp.uomustansiriyah.edu.iq/

Copyright © 2024 *NanoMatImp*. This work licensed under a Creative Commons Attribution Noncommercial 4.0 International License.

[10] M. M. Abhyankar *et al.*, "Optimizing a Multi-Component Intranasal Entamoeba Histolytica Vaccine Formulation Using a Design of Experiments Strategy," (in English), *Frontiers in Immunology*, Original Research vol. 12, 2021. https://doi.org/10.3389/fimmu.2021.683157.

[11] F.-H. Lin *et al.*, "The Epidemiology of Entamoeba histolytica Infection and Its Associated Risk Factors among Domestic and Imported Patients in Taiwan during the 2011–2020 Period," *Medicina*, vol. 58, no. 6, https://doi.org/10.3390/medicina58060820

[12] W. Jing *et al.*, "Serologic diagnosis of Entamoeba histolytica infection based on the gradient-based digital immunoassay," *Analytica Chimica Acta*, vol. 1339, p. 343602, 2025. https://doi.org/10.1016/j.aca.2024.343602.

[13] G. A. Jasim and M. H. Alardi, "Diagnosis and genotyping detection of entamoeba spp. In human and some animals," *International Journal of Research*, vol. 3, no. 12, p. 11-18, 2015.

[14] S. K. Sardar *et al.*, "A New Multiplex PCR Assay Reveals the Occurrence of E. bangladeshi alongside E. histolytica and E. moshkovskii in Eastern India," *Acta Parasitologica*, vol. 69, no. 4, p. 1886-1895, 2024. https://doi.org/10.1007/s11686-024-00921-z.

[15] E. A. Latief, A. T. Mohi, and A. N. Abd, "Effect of Natural Dye on the Spectral Response of the Heterojunction Ag/ZnO/Ps/Si/Ag for Photodetector Application," *International Journal of Nanoscience*, vol. 22, no. 06, p. 2350048, 2023. https://doi.org/10.1142/s0219581x23500485.

[16] F. Esnaashari and H. Zahmatkesh, "Antivirulence activities of Rutin-loaded chitosan nanoparticles against pathogenic Staphylococcus aureus," *BMC Microbiology*, vol. 24, no. 1, p. 328, 2024. https://doi.org/10.1186/s12866-024-03446-7.

[17] A. Y. Madkhli and L. G. Alharbe, "Modified and enhancement polyvinyl alcohol/chitosan (PVA/Cs) films incorporated by hybrid silver tungstate (Ag2WO4) nanoparticles," *Physics Open*, vol. 22, p. 100247, 2025. https://doi.org/10.1016/j.physo.2024.100247.

[18] A. Y. Al-Jumaily, S. S. Al-Jubori, and A. Al-Haddad, "Green synthesized TiO2 nanoparticles impact on extensive-drug resistance gram-negative bacteria," *AIP Conference Proceedings*, vol. 3097, no. 1, p. 020014, 2024. https://doi.org/10.1063/5.0209550.

[19] L. Sun, Y. Su, A. Jiao, X. Wang, and B. Zhang, "T cells in health and disease," *Signal Transduction and Targeted Therapy*, vol. 8, no. 1, p. 235, 2023. https://doi.org/10.1038/s41392-023-01471-y.

[20] L. A. Marcos and E. Gotuzzo, "Intestinal protozoan infections in the immunocompromised host," *Current Opinion in Infectious Diseases*, vol. 26, no. 4, p. 295-301, 2013. https://doi.org/10.1097/QCO.0b013e3283630be3.

[21] J. VENTURA-JUÁREZ *et al.*, "Immunohistochemical characterization of human fulminant amoebic colitis," *Parasite Immunology*, vol. 29, no. 4, p. 201-209, 2007. https://doi.org/10.1111/j.1365-3024.2007.00934.x.

[22] S. Ito *et al.*, "Characterization of colorectal cancer by hierarchical clustering analyses of five immune cell markers," *Pathology International*, vol. 74, no. 1, p. 13-25, 2024. https://doi.org/10.1111/pin.13391.

Downloaded from https://nanomatimp.uomustansiriyah.edu.iq/

Copyright © 2024 *NanoMatImp*. This work licensed under a Creative Commons Attribution Noncommercial 4.0 International License.